

Controllable entanglement and polarization phase gate in coupled double quantum-well structures

Wen-Xing Yang^{1,2} and Ray-Kuang Lee¹

¹*Institute of Photonics Technologies, National Tsing-Hua University, Hsinchu 300, Taiwan*

²*Department of Physics, Southeast University, Nanjing 210096, China*

rklee@ee.nthu.edu.tw

Abstract: By analyzing the nonlinear optical response in an asymmetric coupled double quantum well structure based on the intersubband transitions, we show that a giant Kerr nonlinearity with a relatively large cross-phase modulation coefficient can be used to produce efficient photon-photon entanglement and implement an all-optical two-qubit quantum polarization phase gate. We also demonstrate that such photon-photon entanglement is practically controllable and may facilitate more practical applications in all-optical quantum information and computation.

© 2008 Optical Society of America

OCIS codes: (190.3270) Kerr effect; (270.5585) Quantum information and processing; (190.5970) Semiconductor nonlinear optics including MQW; (230.1150) All-optical devices.

References and links

1. H. C. Liu and F. Capasso, "Intersubband Transitions in Quantum Wells: Physics and Device Applications," (Academic Press, 2000).
2. K. J. Boller, A. Imamoglu, and S. E. Harris "Observation of electromagnetically induced transparency," *Phys. Rev. Lett.* **66**, 2593-2596 (1991).
3. S. E. Harris, "Electromagnetically Induced Transparency," *Phys. Today* **50**, 36-42 (1997).
4. C. Ottaviani, D. Vitali, M. Artoni, F. Cataliotti, and P. Tombesi, "Polarization Qubit Phase Gate in Driven Atomic Media," *Phys. Rev. Lett.* **90**, 197902(1-4) (2003).
5. A. Joshi and M. Xiao, "Phase gate with a four-level inverted-Y system," *Phys. Rev. A* **72**, 062319(1-5) (2005).
6. C. Hang, Y. Li, L. Ma, and G. Huang, "Three-way entanglement and three-qubit phase gate based on a coherent six-level atomic system," *Phys. Rev. A* **74**, 012319(1-7) (2006).
7. H. Schmidt and A. Imamoglu, "Giant Kerr nonlinearities obtained by electromagnetically induced transparency," *Opt. Lett.* **21**, 1936-1938 (1996).
8. P. Ginzburg and M. Orenstein, "Slow light and voltage control of group velocity in resonantly coupled quantum wells," *Opt. Express* **14**, 12467-12472 (2006).
9. H. Schmidt, K. L. Campman, A. C. Gossard, and A. Imamoglu, "Tunneling induced transparency: Fano interference in intersubband transitions," *Appl. Phys. Lett.* **70**, 3455-3457 (1997).
10. C. C. Phillips, E. Paspalakis, G. B. Serapiglia, C. Sirtori, and K. L. Vodopyanov, "Observation of electromagnetically induced transparency and measurements of subband dynamics in a semiconductor quantum well," *Physica E* **7**, 166-173 (2000).
11. L. Silvestri, F. Bassani, G. Czajkowski, and B. Davoudi, "Electromagnetically induced transparency in asymmetric double quantum wells," *Eur. Phys. J. B* **27**, 89-102 (2002).
12. J.-H. Wu, J.-Y. Gao, J.-H. Xu, L. Silvestri, M. Artoni, G. C. La Rocca, and F. Bassani "Ultrafast All Optical Switching via Tunable Fano Interference," *Phys. Rev. Lett.* **95**, 057401(1-4) (2005).
13. P. Palinginis, F. Sedgwick, S. Crankshaw, M. Moewe, and C. Chang-Hasnain, "Room temperature slow light in a quantum-well waveguide via coherent population oscillation," *Opt. Express*. **13**, 9909-9915 (2005).
14. P. C. Ku, F. Sedgwick, C. J. Chang-Hasnain, P. Palinginis, T. Li, H. Wang, S. W. Chang, and S. L. Chuang, "Slow light in semiconductor quantum wells," *Opt. Lett.* **29**, 2291-2293 (2004).

15. W. X. Yang, J. M. Hou, and R.-K. Lee, "Ultraslow bright and dark solitons in semiconductor quantum wells," *Phys. Rev. A* **77**, 033838(1-7) (2008).
16. S. Sarkar, Y. Guo, and H. Wang, "Tunable optical delay via carrier induced exciton dephasing in semiconductor quantum wells," *Opt. Express* **14**, 2845-2850 (2006).
17. H. G. Roskos, M. C. Nuss, J. Shah, K. Leo, D. A. B. Miller, A. M. Fox, S. Schmitt-Rink, and K. Kohler, "Coherent submillimeter-wave emission from charge oscillations in a double-well potential," *Phys. Rev. Lett.* **68**, 2216-2219 (1992).
18. M. S. C. Luo, S. L. Chuang, P. C. M. Planken, I. Brener, and M. C. Nuss, "Coherent double-pulse control of quantum beats in a coupled quantum well," *Phys. Rev. B* **48**, 11043-11050 (1993).
19. P. C. M. Planken, I. Brener, M. C. Nuss, M. S. C. Luo, and S. L. Chuang, "Coherent control of terahertz charge oscillations in a coupled quantum well using phase-locked optical pulses," *Phys. Rev. B* **48**, 4903-4906 (1993).
20. J. Li, "Coherent control of optical bistability in tunnel-coupled double quantum wells," *Opt. Commun.* **274**, 366-371 (2007).
21. J. F. Dynes and E. Paspalakis, "Phase control of electron population, absorption, and dispersion properties of a semiconductor quantum well," *Phys. Rev. A* **73**, 233305(1-4) (2006).
22. J. Faist, C. Sirtori, F. Capasso, S.-N. G. Chu, L. N. Pfeiffer, and K. W. West, "Tunable Fano interference in intersubband absorption," *Opt. Lett.* **21**, 985-988 (1996).
23. G. P. Agrawal, "Nonlinear fiber optics," (3rd ed. Academic Press, New York, 2001).
24. Y. Wu and L. Deng, "Ultraslow optical solitons in a cold four-state medium," *Phys. Rev. Lett.* **93**, 143904(1-4) (2004).
25. M. Fleischhauer, A. Imamoglu, and J. P. Marangos, "Electromagnetically induced transparency: Optics in coherent media," *Rev. Mod. Phys.* **77**, 633-674 (2005).
26. H. Kang, G. Hernandez, and Y. F. Zhu, "Superluminal and slow light propagation in cold atoms," *Phys. Rev. A* **70**, 011801(R)(1-4) (2004).
27. W. K. Wootters, "Entanglement of formation of an arbitrary state of two qubits," *Phys. Rev. Lett.* **80**, 2245-2248 (1998).
28. Y. Wu and X. Yang, "Highly efficient four-wave mixing in double- Λ system in ultraslow propagation regime," *Phys. Rev. A* **70**, 053818(1-5) (2004).
29. I. Waldmüller, J. Forstner, S.-C. Lee, A. Knorr, M. Woerner, K. Reimann, R. A. Kaindl, T. Elsaesser, R. Hey, and K. H. Ploog, "Optical dephasing of coherent intersubband transitions in a quasi-two-dimensional electron gas," *Phys. Rev. B* **69**, 205307(1-9) (2004).
30. D. E. Nikonov, A. Imamoglu, L. V. Butov, and H. Schmidt, "Collective intersubband excitations in quantum wells: Coulomb interaction versus subband dispersion," *Phys. Rev. Lett.* **79**, 4633-4636 (1997).
31. E. Paspalakis, M. Tsaousidou, and A. F. Terzis, "Coherent manipulation of a strongly driven semiconductor quantum well," *Phys. Rev. B* **73**, 125344(1-5) (2006).

There have been many progresses in the development of logic gates and memory devices using nonlinear optical effects, especially with the resonant semiconductor optical nonlinearities [1]. Resonant optical nonlinearities in semiconductors occur at the small intensity and small current, with a controllable flexibility. But the spectral overlap of the absorption and corresponding refractive index changes must be taken into account for such device designs. The existence of the electromagnetically induced transparency (EIT) in systems of semiconductor quantum well (SQW) structures is of particular significance because EIT and EIT-related phenomena have been proven to have a vast number of important applications in cold atom gases [2, 3, 4, 5, 6, 7] and hence received considerable attentions in the past decades. It opens up an avenue to explore new possibilities for nonlinear optics and related quantum information processing (QIP) via EIT. It is more advantageous at least from the view point of practical purposes to find, instead of above mentioned cold atom gases, SQW solid systems to realize giant cross phase modulation (XPM) phase shifts and the related QIP with merits such as large electric dipole moments due to the small effective electron mass, high nonlinear optical coefficients, and a great flexibility in device design by choosing the materials and structure dimensions. Besides, in SQW devices the transition energies, dipoles, and symmetries can also be controlled at will. More importantly, the SQW structure also provides another possibility to realize electrically controlled phase modulators and QIP due to that the conduction subband energy level can be easily tuned by an external bias voltage [8, 9]. In this regards, we note that EIT [10, 11], tunneling-induced transparency (TIT) [9], ultrafast switching [12], slow light [8, 13, 14], optical

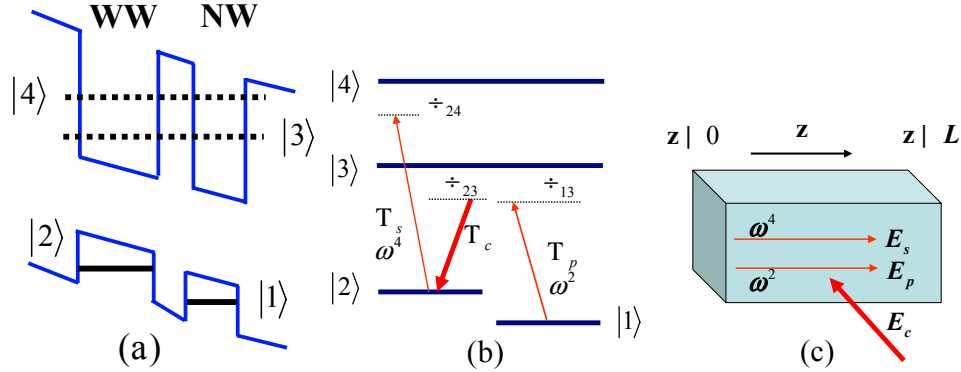


Fig. 1. (a) Schematic band diagram of the asymmetric CQW structure consisting of a wide well (WW) and a narrow well (NW). (b) Schematic of the four-level electronic system synthesized in CQW structure. Ω_p (σ^+ polarization), Ω_s (σ^- polarization), and Ω_c are the Rabi frequencies of the probe, signal, and cw control fields, respectively. The Δ_{ij} denotes the corresponding detunings. (c) Possible arrangement of experimental apparatus. E_c represents the control field and E_p (E_s) represents the σ^+ (σ^-) polarized probe (signal) field, respectively.

solitons [15], optical delay [16], etc, have been investigated in SQW systems. However, as far as we know, up to now no any work has explored Kerr nonlinearity and its applications for producing entangled-photon states and all-optical quantum phase gate (QPG) based on EIT effect in SQW systems.

In this work, we propose a scheme to produce entangled-photon states and implement an all-optical two-qubit QPG through a four-subband N -type system in an asymmetric coupled double quantum well (CQW) structure based on intersubband transitions (ISBT). First, we analyze the nonlinear optical response of the proposed scheme and obtain the optimal conditions to enhance the cross-Kerr nonlinearity significantly and the related XPM with the suppressing of absorption in the medium. Then we study the entangled-photon states and the possibility of employing such enhanced XPM to construct an all-optical two-qubit QPG, in which the binary quantum information is encoded by using the polarization degree of freedom of the probe and signal fields. The results we have obtained here may facilitate more practical applications for QIP in solid media.

1. Model for couple double quantum wells

Let us consider an asymmetric CQW structure [17] consisting of a wide well (WW) and a narrow well (NW) as shown in Fig. 1, where level $|1\rangle$ and level $|2\rangle$ are localized hole states in the valence band. And level $|3\rangle$ and level $|4\rangle$ are delocalized electronic states extended between the wells in the conduction band (a bonding state and an antibonding one), which arise due to the tunneling effect. The system interacts with a weak pulsed probe field of center frequency ω_p , a weak pulsed signal field of frequency ω_s , and a strong continuous wave (cw) control field of frequency ω_c . The Rabi frequencies associated with the lasers driving the transitions are defined as $\Omega_k = \mu_{ij}E_k/\hbar$ ($i, j = 1, 2, 3, 4$ and $i \neq j$), with E_k, μ_{ij} being the corresponding electric field amplitude and the relative dipole matrix element induced on the transition $|i\rangle \leftrightarrow |j\rangle$, respectively. The detunings Δ_{ij} (see Fig. 1) are defined as: $\Delta_{13} = E_3/\hbar - \omega_p$, $\Delta_{23} = (E_3 - E_2)/\hbar - \omega_c$, and $\Delta_{24} = (E_4 - E_2)/\hbar - \omega_s$. Here we have taken $E_1 = 0$ for the ground state level $|1\rangle$ as the energy origin. This CQW structure can be consisted of 10 pairs of a 51-monolayer (145 \AA) thick wide

well and a 35-monolayer (100Å) thick narrow well, separated by an Al_{0.2}Ga_{0.8}As buffer layer. The first ($n = 1$) electron levels in the wide well and the narrow well can be energetically aligned with each other by applying a static electric field, while the corresponding $n = 1$ hole levels are never aligned along this polarization direction of the field. The electrons then delocalize over both wells while the holes remain localized. For transitions from the narrow well and wide well, the Coulomb interaction between the electron and the hole down shifts the value of the electric field, where the resonance condition is fulfilled to the corresponding built-in field. Such a CQW system has been intensively studied previously but in different context [18, 19, 20]. In the present analysis we use the following conditions: (i) The semiconductor quantum wells with low doping are designed such that electron-electron effects have very small influence in our results. As a result, many-body effects arising from electron-electron interactions are not included in our study. (ii) We assume that all subbands have the same effective mass. Working in the interaction picture, utilizing the rotating-wave approximation (RWA) and the electric-dipole approximation (EDA), the dynamics of our system can be described by equations of motion for the probability amplitudes of the electronic wave functions,

$$i\frac{\partial A_1}{\partial t} = \Omega_p^* A_3, \quad (1)$$

$$i\frac{\partial A_2}{\partial t} = (\Delta_{23} - i\frac{\gamma_2}{2})A_2 + \Omega_c^* A_3 + \Omega_s^* A_4, \quad (2)$$

$$i\frac{\partial A_3}{\partial t} = (\Delta_{13} - i\frac{\gamma_3}{2})A_3 + \Omega_p A_1 + \Omega_c A_2 + i\kappa A_4, \quad (3)$$

$$i\frac{\partial A_4}{\partial t} = (\Delta_{24} - i\frac{\gamma_4}{2})A_4 + \Omega_s A_2 + i\kappa A_3, \quad (4)$$

together with A_j ($j = 2, 3, 4$) being the amplitudes of subbands $|j\rangle$. The parameters $\gamma_{2,3,4}$ are added phenomenologically to describe the corresponding decay rates of subbands $|2\rangle$, $|3\rangle$ and $|4\rangle$. The total decay rate γ_i ($\gamma_i = \gamma_{il} + \gamma_i^{dph}$) of subband $|i\rangle$ comprises a population-decay contribution γ_{il} , primarily due to the longitudinal optical (LO) phonon emission events at low temperature, and a dephasing contribution γ_i^{dph} , determined by electron-electron scattering, interface roughness, and phonon scattering processes. The population decay rates can be calculated by solving the effective mass Schrödinger equation. For the temperatures up to 10 K, the electric sheet density kept below $5 \times 10^{11} \text{ cm}^{-2}$ per double well to minimize dephasing from carrier scattering [17], the dephasing decay rates γ_{ij}^{dph} can be estimated according to Refs. [21, 22]. $\kappa = \sqrt{\gamma_{3l}\gamma_{4l}}$ denotes the mutual coupling of states $|3\rangle$ and $|4\rangle$ via the LO phonon decay; it describes the process in which a phonon is emitted by subband $|3\rangle$ and recaptured by subband $|4\rangle$. Such behavior is similar to the decay-induced interference in atomic systems with two closely lying energy states [9].

2. Giant cross-Kerr nonlinearity and group velocity matching

We assume that the initial state of the system is in the ground state $|1\rangle$. Note that if the intensities of the probe and signal fields are much weaker than that of the control field, we can neglect the decay of the ground state due to the quantum coherence and interference effects, thus we can have $A_1 \approx 1$. In other words, the pumping effect among different ground state levels can be neglected during the evolution of the system because almost all electrons will remain in the subband level $|1\rangle$. In order to solve Eqs. (1-4), we assume that the typical operation time durations of the probe and signal fields are long enough so that a steady state approximation can be employed. To obtain the expressions for nonlinear optical susceptibilities of this system we consider higher order contributions to A_1 , which can be obtained by using the normalization condition $\sum_{j=1}^4 |A_j|^2 \approx 1$. By solving Eqs. (1-4) under these conditions, one can obtain

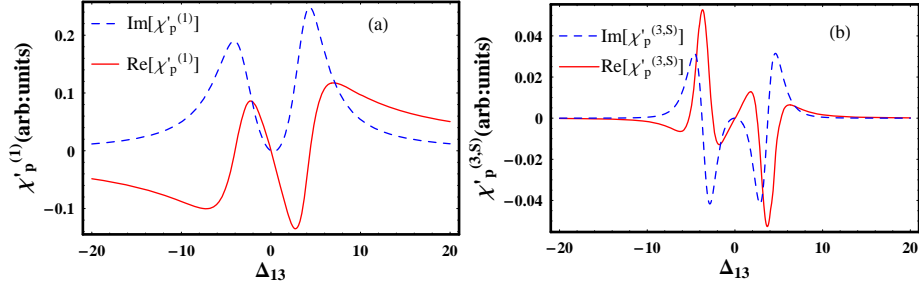


Fig. 2. The real and imaginary parts of (a) the linear susceptibility $\chi_p^{(1)} = N|\mu_{13}|^2/\hbar\epsilon_0\chi_p^{\prime(1)}$, and (b) third-order self-Kerr susceptibility $\chi_p^{(3,S)} = N|\mu_{13}|^4/\hbar^3\epsilon_0\chi_p^{\prime(3,S)}$ versus the detuning of the probe field Δ_{13} (in the unit of meV). Other parameters used here are given by $\gamma_2 = 0$, $\gamma_{3l} = \gamma_{4l} = 3.5\text{meV}$, $\gamma_3^{dph} = \gamma_4^{dph} = 1.5\text{meV}$, $\Delta_{24} = 8\text{meV}$, $\Omega_c = 25\text{meV}$, and $\Omega_s = 2.5\text{meV}$.

$$A_{j=2,3,4} = \frac{(c\Omega_c^* - i\Omega_s^*\kappa)\delta_{j2} + (-bc + |\Omega_s|^2)\delta_{j3} + (ib\kappa - \Omega_c^*\Omega_s)\delta_{j4}}{abc + b\kappa^2 - a|\Omega_s|^2 - c|\Omega_c|^2 + i\kappa(\Omega_c^*\Omega_s + \Omega_c\Omega_s^*)}\Omega_p, \quad (5)$$

where $a = \Delta_{13} - i\gamma_3/2$, $b = \Delta_{23} - i\gamma_2/2$, and $c = \Delta_{24} - i\gamma_4/2$. From above values of A_2 , A_3 , and A_4 , we can obtain the following expressions for the susceptibilities of probe and signal fields, χ_p and χ_s , respectively [23],

$$\chi_p = -\frac{N|\mu_{13}|^2}{\hbar\epsilon_0} \frac{A_3 A_1^*}{\Omega_p} \simeq \chi_p^{(1)} + \chi_p^{(3,S)} |E_p|^2 + \chi_p^{(3,C)} |E_s|^2, \quad (6)$$

$$\chi_s = -\frac{N|\mu_{24}|^2}{\hbar\epsilon_0} \frac{A_4 A_2^*}{\Omega_s} \simeq \chi_s^{(3,C)} |E_p|^2, \quad (7)$$

where N is the electron density in the conduction band of quantum well and ϵ_0 is the vacuum dielectric constant. $\chi_p^{(1)}$, $\chi_p^{(3,S)}$, and $\chi_p^{(3,C)}$ are respectively the linear susceptibility, third-order nonlinear susceptibilities characterizing the effect of self-Kerr and cross-Kerr nonlinearities of the probe field, and $\chi_s^{(3,C)}$ is the third-order cross-Kerr nonlinear susceptibility of the signal field.

With suitable parameters, the associated cross-Kerr susceptibilities $\chi_p^{(3,C)}$ and $\chi_s^{(3,C)}$ can be greatly enhanced under EIT condition. We show in Fig. 2 the linear and self-Kerr susceptibilities versus the probe field for various detunings Δ_{13} under the EIT condition, which illustrates the EIT response of a "Λ-type" subsystem. In the case of resonance of the probe field Ω_p ($\Delta_{13} = 0$), the Λ subsystem forms an dark state where the real and the imaginary parts of both $\chi_p^{(1)}$ and $\chi_p^{(3,S)}$ vanish. Fig. 3 shows the dependence of the third-order cross-Kerr susceptibilities, $\chi_p^{(3,C)}$ and $\chi_s^{(3,C)}$, on the detuning of the signal field Ω_s with the resonance condition of the fields Ω_p and Ω_c (i.e., $\Delta_{13} = \Delta_{23} = 0$). From Fig. 3, one can find that the real parts of the two cross-Kerr susceptibilities decay much more slowly than the imaginary parts within the transparency window. Therefore, when the signal field is relatively far off resonance we can achieve an appreciable XPM phase shift with a negligible absorption. Besides, it is observed that the two cross-Kerr susceptibilities are of the same order of magnitudes. Although it is well known that a similar N-type scheme is analyzed in the cold atom system [7, 24], but different from other systems (such as cold atom gases), here we can obtain very large dipole moments

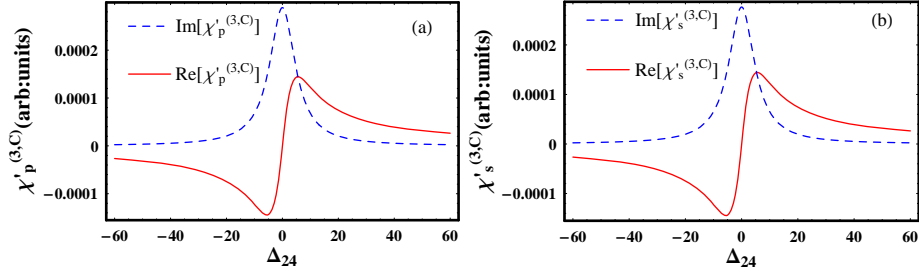


Fig. 3. The real and imaginary parts of the third-order cross-Kerr susceptibilities for (a) the probe field $\chi_p^{(3,C)} = N|\mu_{13}|^2|\mu_{24}|^2/\hbar^3\epsilon_0\chi_p^{\prime(3,C)}$, and (b) the signal field $\chi_s^{(3,C)} = N|\mu_{13}|^2|\mu_{24}|^2/\hbar^3\epsilon_0\chi_s^{\prime(3,C)}$ versus the detunings Δ_{24} (in the unit of meV) at the center of EIT window. Other parameters used are the same as those in Fig. 2.

for the ISBT in our CQW system [17, 18, 19]. For a certain detuning $\Delta_{24} = 10$ meV, it can be calculated that the real part of cross-Kerr susceptibility is about $10^{-10}\text{m}^2\text{V}^{-2}$, which is much larger than that can be achieved in microstructured optical fibers (about $10^{-22}\text{m}^2\text{V}^{-2}$) [23] and in cold atom systems (about $10^{-14}\text{m}^2\text{V}^{-2}$) [24]. Importantly, this is achieved with the linear and self-Kerr interactions vanish simultaneously. This interesting results are produced by the quantum coherence and interference between the lower states under the EIT condition. In addition, one can readily checked that the decay-induced interference, κ , only has a small effect on the XPM because here the XPM is mainly induced by the control field Ω_c under the condition $\kappa \ll \Omega_c$.

It should be emphasized that group velocity matching is another necessary condition to achieve a large mutual phase shift because only in this way can the probe and signal optical pulses interact for a sufficiently long time in a transparent nonlinear medium [4]. The group velocity of an optical pulse is given by $v_g = c/(1 + n_g)$, where c is the speed of light in vacuum, and the group index is given by

$$(n_g)_i = \text{Re}[\chi] + (\omega_i/2)(\partial\text{Re}[\chi]/\partial\omega)_{\omega_i} \quad (8)$$

with ω_i ($i = p, s$) being the laser frequency. We assume that the probe field works at the center of EIT window (i.e., $\Delta_{23} = \Delta_{13} = 0$). Two group velocities, $(v_g)_p$ and $(v_g)_s$, can be made both small and equal by properly adjusting the Rabi frequencies, dipole moments, and detunings. According to the parameters setting above, we show in Fig. 4 the dimensionless group velocities $(v_g)_{p,s}$ of the probe and signal fields versus the detuning Δ_{24} , with $\Omega_p = 4.2$ meV and $\Omega_s = 2.5$ meV. From Fig. 4, one can find that the group velocities of two fields can be matched approximately within the range of detunings $9 \leq \Delta_{24} \leq 10$ meV. As shown in the Fig. 4, the group velocities of both probe and signal fields are reduced with the order of 10^2 in a small range of Δ_{24} . From Fig. 1(b), one can find that Ω_p , Ω_c , and the three levels $|1\rangle$, $|2\rangle$, $|3\rangle$, form a Λ subsystem of the regular EIT configuration. The probe light Ω_p can propagate slowly in this condition. Even there is no population (or negligible population) in state $|2\rangle$, the energy level $|2\rangle$ will be modulated by the strong coupling field Ω_c [25], which will result in the dispersion of field Ω_s . Both Ω_p and Ω_c will contribute to the dispersion, just as Ω_s can affect the dispersion of the probe field Ω_p [26]. Besides, we can obtain large dipole moments in our CQW structure. Thus matched slow light output can exist through suitable parameters.

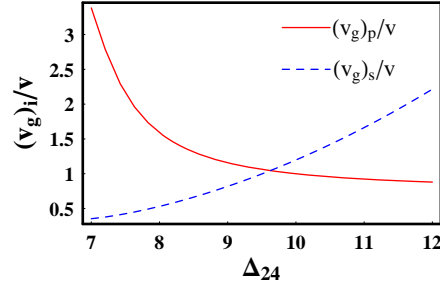


Fig. 4. Dimensionless group velocities $(v_g)_{p,s}/v$ of the probe and signal fields versus the detunings of the signal field Δ_{24} (in the unit of meV) for $v = 10^6$ m/s, in which the solid and dashed lines denote the probe and signal fields, respectively.

3. Controllable entanglement and two-qubit phase gate

In this section, we demonstrate that such third-order cross-Kerr nonlinearity can be used to implement a 2-qubit controlled QPG. A 2-qubit QPG operation can be expressed as $|i\rangle_1 |j\rangle_2 \rightarrow \exp(i\phi_{ij}) |i\rangle_1 |j\rangle_2$, where $i, j = 0, 1$ denote the logical qubit basis. The binary information in our system is encoded by using the polarization degree of freedom in the probe and signal pulses. We assume the four-state system shown Fig. 1 is implemented when the probe field has σ^+ polarization and the signal one has polarization σ^- . If either (both) the probe or (and) the signal polarizations are changed, the phase shifts acquired by two pulses do not involve the cross-Kerr nonlinearity and lead to a difference. Specifically, when probe field has a "wrong" polarizations (σ^- -polarized) there is no sufficiently close excited state to which the subbands can be coupled and the two fields acquire only the trivial phase shift $\phi_0^i = k_i L$ ($i = p, s$) in vacuum, where L is the length of the medium and $k_i = \omega_i/c$ denotes the free space wave vector. When probe and signal fields are both σ^+ -polarized, the probe field, subject to the EIT condition produced by the Λ configuration of $|1\rangle - |2\rangle - |3\rangle$ subbands, experiences a self-Kerr effect and acquires a nontrivial phase shift $\phi_\Lambda^p = \phi_0^p + \phi_1^p + \phi_{3,S}^p$, with $\phi_1^p = 2\pi k_p L \chi_p^{(1)}$ being the linear phase shift and $\phi_{3,S}^p$ begin the nonlinear phase shift induced by self-Kerr nonlinearity (i.e. the self-phase modulation). Moreover, the signal acquires again the vacuum phase shift ϕ_0^s . When both of them have the "right" polarizations (probe σ^+ -polarized and signal σ^- -polarized), the probe and signal fields acquire nontrivial phase shifts $\phi_{total}^p = \phi_\Lambda^p + \phi_{3,C}^p$ and $\phi_{total}^s = \phi_\Lambda^s + \phi_{3,C}^s$, respectively. The nonlinear shifts $\phi_{3,C}^p$ and $\phi_{3,C}^s$ induced by the cross-Kerr nonlinearity (i.e. XPM) are given by

$$\phi_{3,C}^p = k_p L \frac{\pi^{3/2} \hbar^2 |\Omega_s^{peak}|^2}{4 |\mu_{24}|^2} \frac{\text{erf}[\zeta_p]}{\zeta_p} \text{Re}[\chi_p^{(3,C)}], \quad (9)$$

$$\phi_{3,C}^s = k_s L \frac{\pi^{3/2} \hbar^2 |\Omega_p^{peak}|^2}{4 |\mu_{13}|^2} \frac{\text{erf}[\zeta_s]}{\zeta_s} \text{Re}[\chi_s^{(3,C)}], \quad (10)$$

where $\zeta_p = (1 - (v_g)_p/(v_g)_s) \sqrt{2} L / (v_g)_p \tau_p$, and ζ_s can be obtained from ζ_p upon interchanging the indices $p \leftrightarrow s$. Here $\text{erf}[\zeta]$ denotes the error function, and τ_i ($i = p, s$) is the time duration of the pulse. Large nonlinear XPM phase shifts take place for appreciably large values of the real parts of two cross-Kerr susceptibilities, especially when the group velocities of probe and signal fields matched, i.e. as $\zeta_{p,s} \rightarrow 0$, the value of $\text{erf}[\zeta_i]/\zeta_i$ reaches the maximum value $2/\sqrt{\pi}$. The truth table for a polarization 2-qubit QPG using our CQW structure reads in the following,

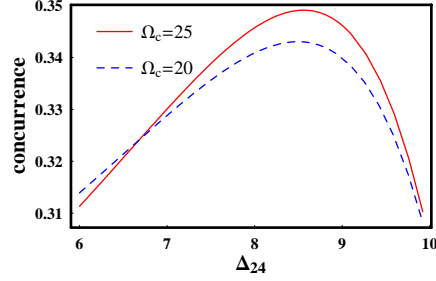


Fig. 5. The concurrence versus the detuning of the signal field (in the unit of meV) for two different Rabi frequencies of control field.

$$|0\rangle_p |0\rangle_s \rightarrow \exp[-i(\phi_0^p + \phi_0^s)] |0\rangle_p |0\rangle_s, \quad (11)$$

$$|0\rangle_p |1\rangle_s \rightarrow \exp[-i(\phi_0^p + \phi_0^s)] |0\rangle_p |1\rangle_s, \quad (12)$$

$$|1\rangle_p |1\rangle_s \rightarrow \exp[-i(\phi_\Lambda^p + \phi_0^s)] |1\rangle_p |1\rangle_s, \quad (13)$$

$$|1\rangle_p |0\rangle_s \rightarrow \exp[-i(\phi_{total}^p + \phi_0^s)] |1\rangle_p |0\rangle_s. \quad (14)$$

Here we have encoded $|\sigma^-\rangle_i \rightarrow |0\rangle_i$ and $|\sigma^+\rangle_i \rightarrow |1\rangle_i$, and the conditional phase shift is $\phi_{con} = \phi_{total}^p + \phi_{total}^s - \phi_\Lambda^p - \phi_0^s$. Based on the above analysis, the linear effect and self-phase modulation can be suppressed when $\phi_\Lambda^p = \phi_0^p$, i.e. $\phi_{total}^p = \phi_0^p + \phi_{3,C}^p$, $\phi_{total}^s = \phi_0^s + \phi_{3,C}^s$, and $\phi_{con} = \phi_{3,C}^p + \phi_{3,C}^s$. In this case, only the third order nonlinear phases in Eqs. (9) and (10) contribute to the conditional phase shift ϕ_{con} . Thus we have realized a 2-qubit polarization phase gate operation in the CQW structure.

We now turn to the problem of entangled-photon states in our quantum well system. Here we use the entanglement of formation as a measurement of the purity in our two polarized photons state. For an arbitrary two-qubit system, the degree of entanglement is defined by [27]

$$E_F(C) = h\left(\frac{1 + \sqrt{1 - C^2}}{2}\right), \quad (15)$$

where $h(x) = -x \log_2(x) - (1-x) \log_2(1-x)$ is Shannon entropy function, and the so called "concurrence", C , is given by

$$C(\hat{\rho}) = \max\{0, \lambda_1 - \lambda_2 - \lambda_3 - \lambda_4\}, \quad (16)$$

with λ_i ($i = 1, 2, 3, 4$) being the square roots of the eigenvalues, in a decreasing order, for the matrix $\hat{\rho} \hat{\sigma}_y^p \otimes \hat{\sigma}_y^s \hat{\rho}^* \hat{\sigma}_y^p \otimes \hat{\sigma}_y^s$. Here $\hat{\rho}^*$ denotes the complex conjugation of the output state density matrix $\hat{\rho}$, and $\hat{\sigma}_y^i$ ($i = p, s$) is the y -component of the Pauli matrix. $E_F(C)$ is a monotonic function of C , thus we can also use the concurrence directly as our measurement of entanglement. It should be emphasized that the entanglement can be controlled by adjusting the related parameters of the system. As an example, we plot in Fig. 5 the concurrence as a function of the detuning Δ_{24} in the unit of meV. For the sake of simplicity, we take the value of $N |\mu_{13}|^2 \omega_p / 2\hbar\epsilon_0 c = N |\mu_{24}|^2 \omega_s / 2\hbar\epsilon_0 c = 10^5$ meV/cm and the length of the medium $L \approx 2$ mm as an example. The probe and signal fields have a mean amplitude about one photon when the beams are tightly focused. For a certain detuning of the signal field ($\Delta_{24} = 10$ meV), we obtain the degree of entanglement $E_F \approx 31\%$ with the conditional phase shift $\phi_{con} \approx \pi$ at the same time. By choosing an appropriate detuning, the maximum degree of entanglement obtained in

our proposal can be as large as 35%. It is worth to note that the fluctuations of light intensities and the detunings of probe and signal fields will result in errors of measurement of the nonlinear phase shift in the experimental demonstration.

4. Discussion and conclusion

Just as done before [12, 15, 20], we analyzed the nonlinear response by using the one-dimensional model in calculation and neglected the momentum dependency of subband energies. However, there is no large discrepancy between the reduced one-dimensional and a full two-dimensional calculations [12]. In addition, we have not used the density matrix formalism including the decay rates to describe the system. It can readily be checked by numerical simulations that the results of the treatment here are essentially the same as those from the usual density matrix formalism [24, 28].

Before conclusion, we should note that we have neglected other additional broadening induced by the carrier-carrier and carrier-photon interactions. In the present one-dimensional model, the effects of additional broadening can be included by first rewriting the corresponding detunings, i.e., $\Delta_{ij} = (E_j - E_i)/\hbar - \omega_{s,p,c}$ as $\Delta_{ij} + \Delta_{ad}$ with Δ_{ad} being the additional broadening effects. According to the Ref. [29], we find that even for the moderate density at 300K, additional broadening effects are on the order of 1 meV, which is very small compared with the final linewidth even at room temperature. Besides, some other many-body effects also contribute to the broadening, for example, the depolarization effect, which renormalizes the free-carrier and carrier-field contributions [30, 31]. Due to the small electron sheet density considered here, these effects only give a small extent.

In conclusion, we have analyzed the nonlinear response of an asymmetric CQW structure based on the intersubband transitions (ISBT). Under the condition $\Delta_{13} = \Delta_{23} = 0$, we have shown that the cross-Kerr susceptibilities can greatly enhanced while the linear and the self-Kerr nonlinear susceptibilities are simultaneously suppressed due to the quantum interference effect induced by a strong cw control laser field. Based on such important features we have studied the entanglement between two weak lights and explored the possibility to implement a robust two-qubit QPG with the given system.

In the literature several four- or multiple-level structures in atomic systems, such as "M-type" or "Y-type", have been proposed to investigate the Kerr nonlinearities [4, 5, 6]. Even in CQW system, this is achieved by mapping the model describing the four subbands interacting with the three laser fields into the model describing the nonlinear response through the gas of four-level cold atoms [7, 24, 28]. However, there are some crucial differences between these two situations, with important implications to be explained shortly. First, the medium studied here is a solid, which is much more practical than that in gaseous media due to its flexible design and the controllable interference strength. Second, the transition energies, dipoles, and symmetries can be controlled at will. For instance, the XPM phase shifts obtained here and the condition of the group velocity matching can be conveniently adjusted within a large range of parameters in a typical CQW system while they can hardly be found in the models for cold atom media. What is more important, the results obtained in the present study may be useful for guiding experimental realization of electrooptically modulated devices and facilitating more practical applications in solid quantum information and computation.

Acknowledgment

We would like to thank Ite. Yu and KaiJun. Jiang for many helpful discussions. The research is supported in part by the National Science Council of Taiwan under the contract number 95-2112-M-007-058-MY3 and NSC-95-2120-M-001-006. WXY is also supported by National Natural Science Foundation of China under Grant Nos. 10704017 and 10575040, by National

Fundamental Research Program of China 2005CB724508.